JOURNAL OF PHYSICAL ORGANIC CHEMISTRY, VOL. 7, 534–544 (1994)

SYNTHESIS AND PHOTOPHYSICS OF DIAZA-CROWN ETHER-BASED BISPORPHYRINS

JERKER MÅRTENSSON*

Department of Organic Chemistry, Chalmers University of Technology, S-412 96 Göteborg, Sweden

KJELL SANDROS

Department of Physical Chemistry, Chalmers University of Technology, S-412 96 Göteborg, Sweden

AND

OLOF WENNERSTRÖM

Department of Organic Chemistry, Chalmers University of Technology, S-412 96 Göteborg, Sweden

The bisporphyrin *N,N'*-bis[4''-(*meso*-triphenylporphyrinyl)benzyl]-4,13-diaza-18-crown-6 and its mono- and dizinc derivatives were synthesized in 66%, 46% and 53% yields, respectively, from 5-(4'-bromomethylphenyl)-10,15,20-triphenylporphyrin or its zinc derivative and 4,13-diaza-18-crown-6. The zinc-containing bisporphyrins form dimers in solution at low temperature or at high concentration. The unsymmetrical bisporphyrin; monozinc *N,N'*-bis[4''-(*meso*-triphenylporphyrinyl)benzyl]-4,13-diaza-18-crown-6 shows singlet–singlet energy transfer from the zinc porphyrin moiety to the free base moiety in both the monomeric and the dimeric form. The energy transfer rates were determined using time-resolved fluorescence spectroscopy and were found to be $1{\cdot}26 \times 10^9$ and $2{\cdot}29 \times 10^9$ s^{-1} for the monomeric and dimeric form, respectively. The difference in energy transfer rates between the two forms can be rationalized by the difference in overlap between the donor fluorescence spectrum and acceptor absorption spectrum, donor–acceptor distance and donor–acceptor orientation.

INTRODUCTION

The theory of radiationless energy transfer was developed by Förster,[1] who introduced a dipole–dipole interaction mechanism for energy transfer referred to as a 'Förster, resonance or Coulomb-type' mechanism, This theory was later extended by Dexter[2] to include higher order multipole interactions and exchange interactions. Energy transfer through exchange interactions is referred to as 'Dexter-type' energy transfer. The Förster mechanism operates via Coulombic interactions between transition moments and does not require physical contact between the donor and acceptor and is, therefore, a long-range mechanism. The Dexter mechanism, on the other hand, operates via electron exchange and thus requires orbital overlap and physical contact between the donor and acceptor and is, therefore, a short-range mechanism. Depending on which mechanism is in operation, the theories predict how the energy transfer rate depends on a variety of parameters, such as distance, relative orientation and energetics within the donor–acceptor system.

In order to confirm these theories and to mimic biological processes in which energy transfer plays a crucial role, a large number of donor–acceptor systems have been prepared and studied. Studies of these donor–acceptor systems have to a large extent confirmed the distance[3] and orientation[4] dependence and also the dependence of energetics[5] and spectral overlap between donor fluorescence and acceptor absorption.

The above theories are intended for the general case of a pair of molecules, a donor and an acceptor, in solution, but are also applicable to the case where the donor and acceptor are held together by electrostatic interactions or intermolecular forces. They are, however, not directly applicable to the case where the donor and acceptor are covalently linked to each other. Recently, energy transfer was shown to be mediated by σ-bonds over much larger distances than predicted by the simplest form of Dexter theory, and to be dependent on the conformation of the chain connecting the donor and acceptor, long-range Dexter.[6] How the

* Author for correspondence.

CCC 0894–3230/94/100534–11

Received 23 August 1993
Revised 9 May 1994

energy transfer rate depends on the electronic structure of the intervening media (solvents, proteins and connecting bridges) is not easily predicted.

In this paper we present the synthesis of and spectroscopic data for a model compound that we hope will enable us to study energy transfer and how it is dependent on the electronic structure of the intervening medium between donor and acceptor. In this model system different groups should be incorporated between donor and acceptor by host–guest complexation. This has the advantage that it makes it possible to study a large number of different groups with a minimum of synthetic work. The model compound is a bisporphyrin consisting of a diaza-crown ether substituted at each nitrogen with a porphyrin unit. The porphyrins may be either identical or different (Figure 1, **1**–**3**). The diaza-crown ethers bind a primary alkylammonium salt and by varying the alkyl group in this salt it should be possible to study how the rate of the energy transfer depends on the physical and chemical properties of the medium between the porphyrins.

In the course of this study a paper was published which presents a system that makes use of the same principle in electron transfer studies.[7] Different cations were complexed into a donor–acceptor system and the effect on the photo-induced electron transfer rate between the donor and the acceptor was studied.

Both at high concentrations and in dilute solutions at low temperature compounds **2** and **3** form dimers held together by nitrogen to zinc coordination.[8] In this ensemble of four porphyrins the mutual distance and orientation and the spectral overlap are drastically changed in comparison with the monomeric form. Photophysical properties of these dimers will also be presented.

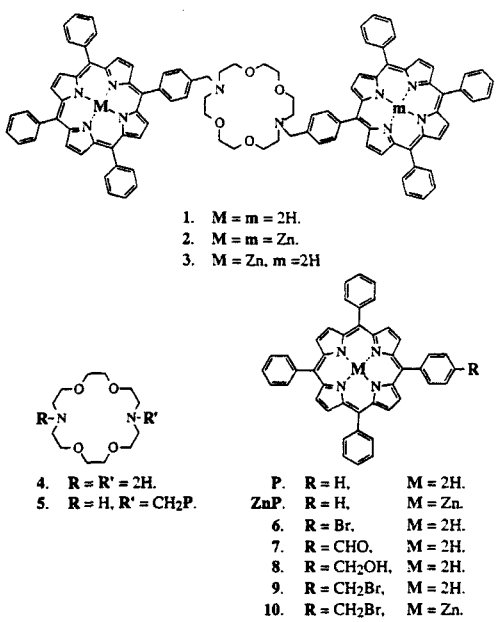

Figure 1. Compounds prepared and used in this study

RESULTS

Synthesis of bisporphyrins 1–3

Porphyrin **6** (Scheme 1) was obtained as the major component in a mixture of six porphyrins with zero to four bromo substituents by condensation of pyrrole with a 3 : 1 molar ratio of benzaldehyde and 4-bromobenzaldehyde according to the Adler–Longo procedure.[9] The porphyrin mixture was treated with butyllithium (BuLi) followed by *N*,*N*-dimethylformamide (DMF) and hydrolysis to yield the formylated porphyrin **7**, contaminated with a small amount of the corresponding chlorin, in 6% yield after chromatography based on the amount of pyrrole used in the condensation step. The chlorin was converted into porphyrin by treatment with 2,3-dichloro-5,6-dicyano-1,4-benzoquinone (DDQ).[10] Aldehyde **7** was then reduced to alcohol **8** with sodium borohydride in 97% yield, which was subsequently converted into bromide **9** in 99% yield by treatment with hydrobromic acid in acetic acid. The bromomethylporphyrin **9** was converted into the corresponding zinc porphyrin in 99% yield by treatment with zinc acetate dehydrate according to the usual metallation procedure.[11] Bisporphyrins **1** and **2** were prepared by *N*,*N*′-dialkylation of 4,13-diaza-18-crown-6 (**4**) with the appropriate porphyrin **9** or **10** in the presence of sodium hydroxide in 66% and 53% yield, respectively. The unsymmetrical bisporphyrin **3** was

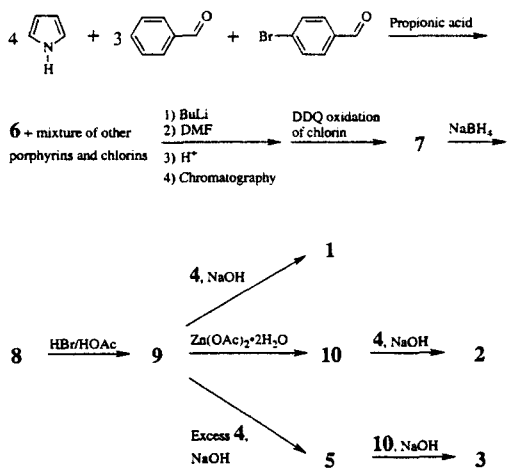

Scheme 1. Synthetic routes to bisporphyrins **1**–**3**

prepared in a two-step *N*-alkylation of diaza-crown ether **4**. In the first step porphyrin **9** was treated with a large excess of diaza-crown ether **4** in the presence of sodium hydroxide to yield the monoalkylated diaza-crown ether **5** in 65% yield based on the amount of **9** used. In the second step bisporphyrin **3** was obtained in 46% yield from **5** by treatment with zinc porphyrin **10** in the presence of sodium hydroxide.

Photophysical properties of the monomeric bisporphyrins 1–3

The ground-state absorption spectra, at 298 K, of the bisporphyrins **1**–**3** in the *Q*-band can be adequately described using a simple sum of the spectra of the individual chromophores, but those in the *B*-band show some small broadening, indicating very small or no interaction in the S_1 states but some small excitonic interaction in the S_2 states between the two porphyrins.[12] This shows that there is a large centre-to-centre distance between the porphyrins consistent with an extended conformation of the bisporphyrins.

The steady-state fluorescence emission spectra were obtained by excitation at 548 nm, which corresponds to the $Q_y(0,0)$-band and $Q(0,1)$-band of the free base porphyrin (P) and the zinc porphyrin (ZnP), respectively. At this excitation wavelength 73% of the light is absorbed by the ZnP moiety in bisporphyrin **3** and also in a 1 : 1 molar mixture of P and ZnP, and the remaining 27% of the light is absorbed by the P. The symmetrical bisporphyrins **1** and **2** gave emission spectra identical with that of P (λ_{max} = 654 and 720 nm) and ZnP (λ_{max} = 598 and 646 nm), respectively. For the unsymmetrical bisporphyrin **3**, the emission spectrum shows three peaks, a small peak at 598 nm and two larger peaks at 652 and 720 nm. This emission spectrum, in contrast to the absorption spectrum of **3**, is not equivalent to the sum of the emission spectra of the individual chromophores. The fluorescence intensity of the ZnP moiety is decreased and that of the free base P moiety is increased, compared with the fluorescence spectrum of a 1 : 1 molar mixture of ZnP and P [Figure 2(a)]. This is consistent with singlet excitation energy transfer from the ZnP moiety to the P moiety in bisporphyrin **3**. This is also shown by the excitation spectrum where the fluorescence intensity at 720 nm, which is due only to the P moiety, is monitored as a function of the excitation wavelength. This spectrum resembles the absorption spectrum, which means that excitation of the ZnP moiety leads to emission from the P moiety or, in other words the ZnP moiety, the donor, transfers its excitation energy to the P moiety, the acceptor.

For excitation at 548 nm of oxygen-free dichloromethane solutions at 298 K, the total fluorescence quantum yields, Φ_f, were found to be 0·100, 0·027, 0·050, 0·098 and 0·083 for P, ZnP, a 1 : 1 molar mixture of P and ZnP, **1** and **3**, respectively. At the concentration of porphyrin used in these measurements ($< 8 \times 10^{-5}$ M) there will be negligible intermolecular energy transfer since the average separation distance is >27 nm.

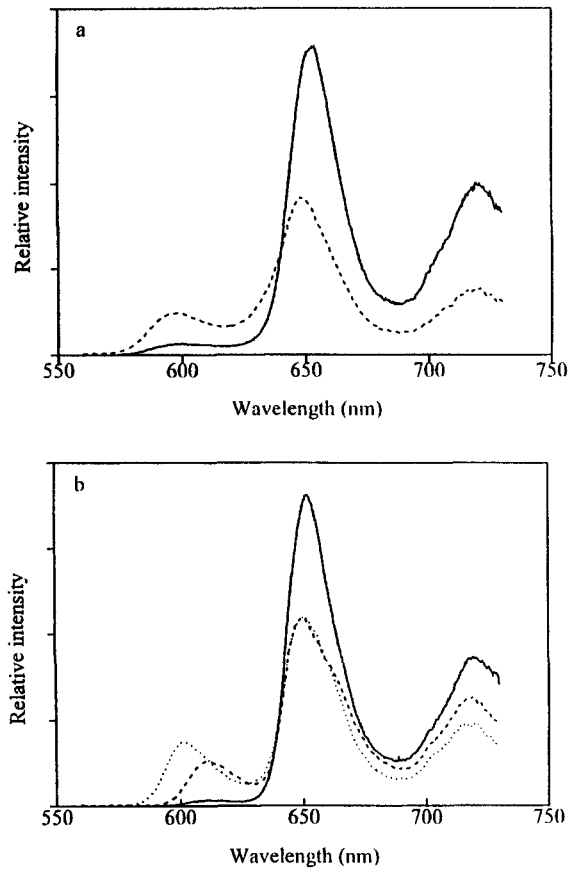

Figure 2. Corrected emission spectra of **3** and a 1 : 1 molar mixture of ZnP and P. (a) solid line, **3**; dashed line, 1 : 1 molar mixture of ZnP and P in CH_2Cl_2 at 298 K. (b) Solid line, **3**; dotted line, 1 : 1 molar mixture of ZnP and P in CH_2Cl_2; dashed line, 1 : 1 molar mixture of ZnP and P in 0·07 M pyridine–CH_2Cl_2 at 190 K

Emission and non-radiative decay from the singlet excited state of the ZnP moiety in **3** will compete with the intramolecular singlet energy transfer. If one assumes that the rates for the two first processes are the same as in ZnP, the quantum yield of the energy transfer, (Φ_{EnT}, can be determined from the fluorescence spectra by using the equation[13]

$$\Phi_{EnT} = 1 - \frac{I_{3(598)}}{I_{ZnP(598)}} \quad (1)$$

where $I_{3(598)}$ = fluorescence intensity at 598 nm for **3**

Table 1. Fluorescence lifetimes of ZnP, **1** and **3** in CH_2Cl_2 at two different temperatures according to time-resolved fluorescence measurements

	298 K		190 K	
Compound	τ_1 (ns)	τ_2 (ns)	τ_1 (ns)	τ_2 (ns)
ZnP	1·80		2·04	
1	8·90		8·80	
3	0·55	8·82	0·36	8·87

and $I_{ZnP(598)}$ = fluorescence intensity at 598 nm for ZnP in the 1 : 1 molar mixture of ZnP and P. This gives the quantum yield for singlet energy transfer in **3** as 0·66.

The results of fluorescence decay measurements are summarized in Table 1. ZnP and **1** show monoexponential fluorescence decays, whereas **3** shows biexponential fluorescence decay.

If one assumes that the shortening of the lifetime (at 298 K) of the ZnP moiety first excited singlet state in **3** is due only to energy transfer, then the rate of the intramolecular singlet energy transfer, k_{EnT}, can be calculated to be $1{\cdot}26 \times 10^9\ s^{-1}$ from these data according to the equation

$$k_{EnT} = \frac{1}{\tau_{S1ZnP(3)}} - \frac{1}{\tau_{S1ZnP}} \qquad (2)$$

where $\tau_{S1ZnP(3)}$ = fluorescence lifetime of the ZnP moiety in bisporphyrin **3** and τ_{S1ZnP} = fluorescence lifetime of ZnP. The quantum yield, Φ_{EnT}, of the energy transfer is given by the equation

$$\Phi_{Ent} = \tau_{S1ZnP(3)} k_{EnT} \qquad (3)$$

and equals 0·69, which is close to the value calculated from equation (1) (0·66).

Photophysical properties of the dimers of bisporphyrins 2 and 3

The ground-state absorption spectra at 190 K, of the dimer of bisporphyrin **3** can be adequately described by a simple sum of the spectra, at the corresponding temperature, of P and nitrogen (pyridine)-coordinated ZnP. No further broadening of the absorption bands due to the dimerization can be observed, in comparison with the bisporphyrins **2** and **3**, which indicates a very small excitonic interaction between the porphyrins in the dimer as in the monomers.

The steady-state fluorescence emission spectra were obtained by excitation at 548 nm. For the dimer of the unsymmetrical bisporphyrin **3**, the emission spectrum shows three peaks, a small peak at 610 nm, even smaller than for the bisporphyrin **3** at 298 K, and two larger peaks at 650 and 717 nm. The fluorescence intensity of the ZnP moiety is decreased and that of the free base P moiety is increased compared with the fluorescence spectrum of the bisporphyrin **3** (Figure 2).

Biexponential fluorescence decay was observed at 190 K. The rate of the intramolecular singlet energy transfer in the dimer of the bisporphyrin **3** is calculated from the fluorescence lifetimes at 190 K given in Table 1 to be $2{\cdot}29 \times 10^9\ s^{-1}$ according to equation (2). The quantum yield of the energy transfer, given by equation (3), equals 0·82.

DISCUSSION

Theoretical aspects of the energy transfer rate in the monomeric bisporphyrin 3

The three-dimensional structure of the bisporphyrin **3** in solution is most likely a rather extended conformation (Figure 3), similar to the solid-state structure found for *N,N'*-bis(benzyl)-4,13-diaza-18-crown-6.[14] This assumption is consistent with the observed shifts of the resonance peaks of the crown ether protons in NMR and that no or very small exciton coupling is seen in the UV–visible spectra of **3**.

The distance between the centre of mass of the donor and acceptor in the structure shown in Figure 3 was estimated from molecular models and by molecular mechanic calculations (MM2) to be 27 Å. The most probable mechanism for energy transfer over such a large distance is the dipole–dipole Förster mechanism. The energy transfer rate can according to the Förster theory be calculated from the equation

$$k_{Ent} = \frac{9(\ln 10)}{128\pi^5 N} \frac{\kappa^2 \Phi_{fZnP}}{n^4 \tau_{S1ZnP} R_{DA}^6} J_{Förster}$$

$$= 8{\cdot}8 \times 10^{-28} \frac{\kappa^2 \Phi_{fZnP}}{n^4\ \tau_{S1ZnP} R_{DA}^6} J_{Förster} \qquad (4)$$

where Φ_{fZnP} and τ_{S1ZnP} are the fluorescence quantum yield and the fluorescence lifetime (in seconds) of the isolated donor, respectively, N is Avogadro's number, n is the solvent refractive index, R_{DA} is the distance (in cm) between the centre of masses of the donor and acceptor, $J_{Förster}$ is the so-called overlap integral and κ^2 is an orientation factor.

The overlap integral, $J_{Förster}$, depends on the spectral overlap between the donor fluorescence and the acceptor absorption according to the equation

$$J_{Förster} = \frac{\int F_D(\nu)\varepsilon_A(\nu)\nu^{-4}\,d\nu}{\int F_D(\nu)\,d\nu} \qquad (5)$$

where $F_D(\nu)$ and $\varepsilon_A(\nu)$ are the fluorescence intensity of the donor and the molar absorptivity (in $l\,mol^{-1}\,cm^{-1}$) of the acceptor as functions of the wavenumber, ν (in cm^{-1}), respectively. $J_{Förster}$ was calculated from

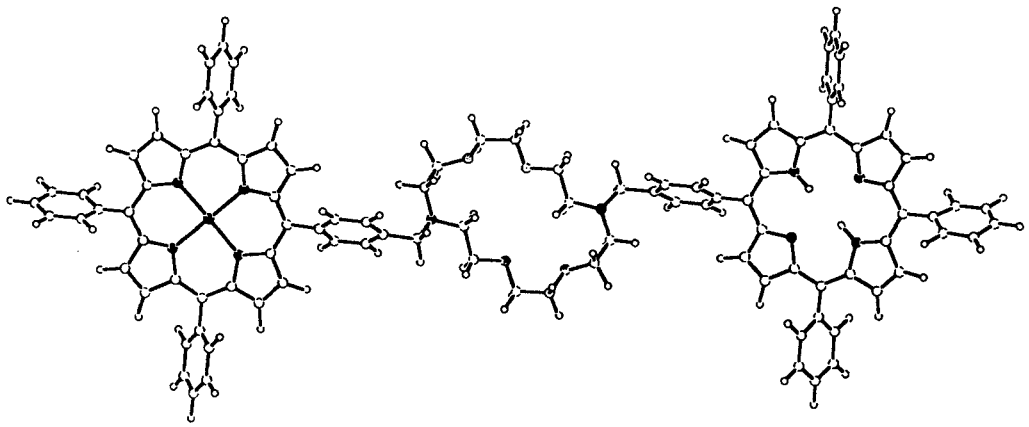

Figure 3. An extended conformer of bisporphyrin **3** derived from the solid-state structure of *N,N'*-bis(benzyl)-4,13-diaza-18-crown-6

our experimental data [Figure 4(a)] to be $3{\cdot}5 \times 10^{-11}$ $cm^6\ mol^{-1}$, which is in good agreement with calculations of $J_{Förster}$ for related systems found in the literature.[4,13,15]

The orientation factor, κ^2, can be calculated according to the equation

$$\kappa^2 = (\cos\gamma - 3\cos\alpha\cos\beta)^2 \qquad (6)$$

where α and β are the angles between the transition dipole moments, in the donor and acceptor, and the vector adjoining the centre of mass of the donor and acceptor, respectively, and γ is the angle between the transition dipole moments. Since there are fast conformational changes, compared with the energy transfer time-scale, in this non-rigid molecule, the measured lifetime of the singlet excited state of ZnP moiety in **3** should be considered as an averaged lifetime of a large number of slightly different donor–acceptor systems with respect to the molecular conformation. The energy transfer rate, calculated from the experimental data, should then be taken as an averaged rate for energy transfer in several possible conformers. This also implies that κ^2 and R_{DA}, used when calculating the theoretical energy transfer rate, should be averaged values of all possible orientation factors and donor–acceptor distances, respectively.

The orientation factor is usually assumed to be constant in the wavelength interval where the donor fluorescence and acceptor absorption overlap, i.e. the orientation of the transition dipole moment is independent of which vibrational states are involved in the transitions. This is not fully correct, however, for the system studied.[12i,16] Further, in ZnP the Q_x and Q_y transitions are degenerate and the system should be treated as a planar oscillator.[16] No corrections are made for the wavelength dependence but the degeneracy of the Q_x and Q_y transitions in ZnP is taken into account when calculating κ^2.

An averaged value of all possible orientation factors is not easily obtained. However, an estimation of in which range κ^2 can be found was obtained from molecular models and molecular mechanics. In order to simplify the estimations of κ^2 for the bisporphyrin **3**, it was assumed that the diaza-crown ether is a rigid segment and that there is free rotation between this segment and the porphyrins. From this model κ^2 was estimated to be in the range 0·8–1·0. R_{DA} is the same for all conformations in this simple model.

Insertion of the obtained values for $J_{Förster}$ and the limits for κ^2 into equation (4) gave the theoretical energy transfer rate to be in the range $(0{\cdot}23–0{\cdot}29) \times 10^9\ s^{-1}$, which is considerably smaller than the experimental value for energy transfer rate in the bisporphyrin **3**. This implies that the simple model of the bisporphyrin used for the calculations of κ^2 is too conformationally restricted and that the average donor–acceptor distance should be shorter than 27 Å. The fact that the donor should be looked at as a planar oscillator implies that even moderate conformational changes during the excited donor lifetime will give a dynamic average κ^2 that can be fairly accurately approximated with the isotropic dynamic average value of 2/3.[2a] The isotropic dynamic average value applies to a system where the donor and acceptor transition dipoles sample all orientations several times during the donor lifetime. If κ^2 is taken to be 2/3 then the experimental energy transfer rate corresponds to an average donor–acceptor distance of 20 Å. The bisporphyrin has to be much more flexible than the simple model used above to be able to achieve this average donor–acceptor distance. This is also supported by MM2 calculations on *N,N'*-bis(benzyl)-4,13-diaza-18-crown-6, which show that various conformers have similar energy.

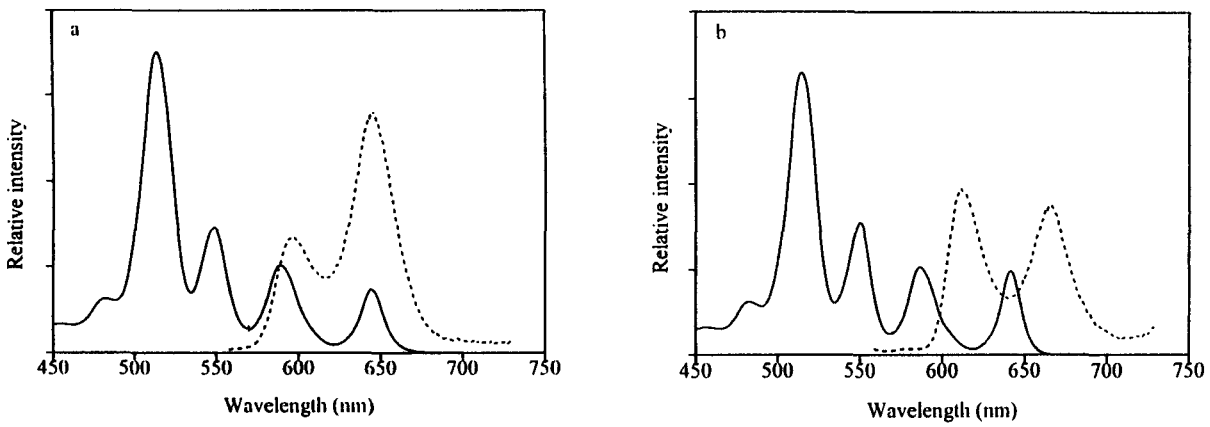

Figure 4. (a) Spectral overlap between ZnP fluorescence (dashed line) and P absorption (solid line) at 298 K in CH_2Cl_2. (b) Spectral overlap between fluorescence from pyridine-coordinated ZnP in 0·07 M pyridine–CH_2Cl_2 (dashed line) and P absorption (solid line) in CH_2Cl_2 at 190 K

Theoretical aspects of the energy transfer rate in the dimer of bisporphyrin 3

The suggested structure of the dimer of the porphyrin is shown in Figure 5.[8] In this ensemble of four porphyrins there are two possible energy transfer pathways. The shorter one is the intermolecular pathway from the donor in one of the two bisporphyrins forming the dimer to the acceptor in the other bisporphyrin. This donor–acceptor distance is 12 Å. The longer pathway is intramolecular and the donor–acceptor distance is 21 Å. Estimations of the orientation factors for the two pathways were made. In the model used for these estimations it is assumed that the segment con-

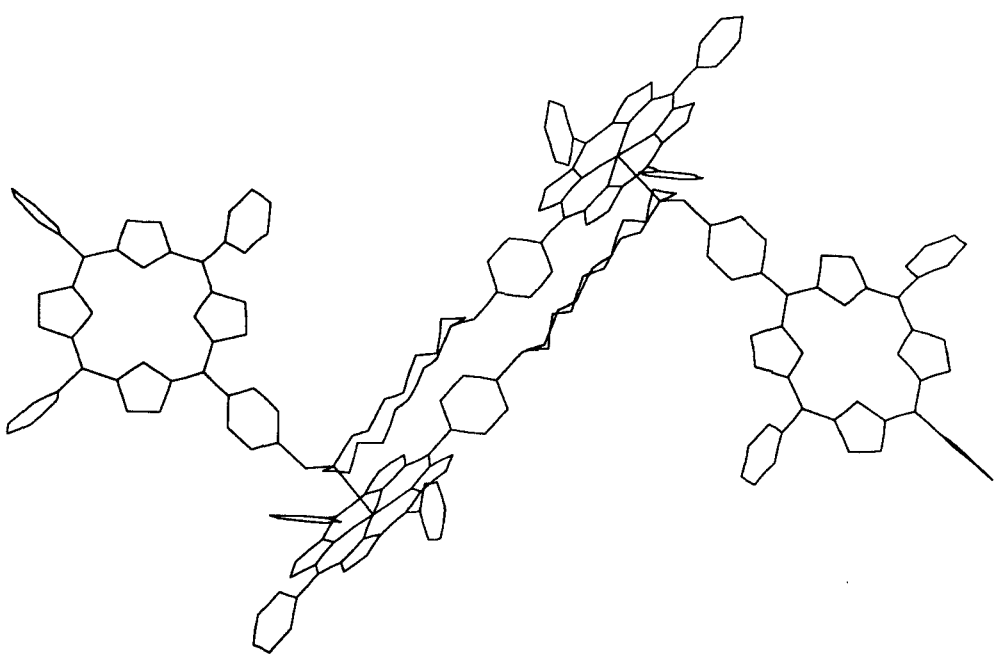

Figure 5. Tentative structure, with a centre of inversion, of the dimer of bisporphyrin 3

taining the two ZnP and the two diaza-crown ethers is rigid and that there is free rotation between this segment and the free base P. κ^2 was then found to be in the range 0·04–0·4 and 0·01–1·4 for the shorter and longer distance, respectively.

Not only are the distance and the relative orientation between donor and acceptor changed relative to the monomeric bisporphyrin **3**, but also the spectral overlap between donor fluorescence and acceptor absorption. The spectral overlap is changed owing to the red shift of ZnP fluorescence when coordinating with a nitrogen ligand. $J_{\text{Förster}}$ was approximated with the overlap between the fluorescence of pyridine-coordinated ZnP and free base P absorption and found to be $1{\cdot}40 \times 10^{-11}$ cm^6 mol^{-1}.

Calculations gave the energy transfer rates for the shorter and the longer path way to be in the range $(0{\cdot}53–5{\cdot}3) \times 10^9$ and $(0{\cdot}005–0{\cdot}65) \times 10^9$ s^{-1}, respectively. The experimental energy transfer rate, $2{\cdot}29 \times 10^9$ s^{-1}, falls well into the interval calculated for the intermolecular pathway. This is an additional support for the suggested structure of the dimer. At such a short distance as 12 Å (seven bonds, including the zinc-to-nitrogen coordination bond, between the donor and acceptor) an additional channel for energy transfer may be opened by the (long-range) Dexter exchange mechanism,[6] or higher order multipole interactions. From the experimental data obtained it is not possible to tell whether these mechanisms contribute to the observed energy transfer rate.

CONCLUSION

A donor–acceptor system showing energy transfer properties and having the ability to complex cations has been synthesized. The energy transfer efficiency in this system was found to be 0·7. This is well suited for our intention to use the system in a study of how the energy transfer depends on the electronic structure of the intervening medium between donor and acceptor, since both an increase and decrease in energy transfer efficiency should be detectable.

We found that in order to obtain agreement between the experimental energy transfer rate and the rate predicted by the Förster theory, it was necessary to assume a fairly large flexibility in the monomeric form of the donor–acceptor system. However, the system should be structurally more well defined when binding a guest by the diaza-crown ether unit.

As already reported,[8] the donor-acceptor system forms a well-ordered ensemble of four porphyrins on dimerization at high concentration or at low temperature. This energy transfer study has given additional support for the formation of a dimer and the suggested structure of the porphyrin ensemble. The energy transfer efficiency in this system was found to be 0·8. The difference in energy transfer efficiency between the monomer and dimer was explained by the difference in overlap between the donor fluorescence spectrum and acceptor absorption spectrum, donor–acceptor distance and donor–acceptor orientation.

Further studies of this donor–acceptor system and the influence on the energy transfer on incorporation of different hydrocarbon groups between the donor and acceptor by complexation are in progress.

EXPERIMENTAL

Materials. All solvents, except chloroform and propionic acid, were distilled prior to use. Diethyl ether and tetrahydrofuran were dried by distillation over sodium–benzophenone ketyl and *N,N*-dimethylformamide was dried by distillation over calcium hydride. The dry solvents were used immediately after distillation. Unless stated otherwise, all commercially available reagents were used without further purification. Silica gel 60 (230–400 mesh) and activated neutral aluminium oxide (Brockmann I, 150 mesh) were used for column chromatography. Thin-layer chromatography (TLC) was performed on commercially prepared silica gel plates coated with silica gel 60 F_{254} and aluminium oxide plates coated with neutral aluminium oxide 60 F_{254} type E. *meso*-Tetraphenylporphyrin (P) was prepared according to the Adler–Longo procedure[9] and purified to remove *meso*-tetraphenylchlorin according to the dry column chromatographic method described by Adler *et al.*[10b,17] The zinc complex of *meso*-tetraphenylporphyrin (ZnP) was prepared by adding zinc acetate dihydrate in methanol to a boiling solution of *meso*-tetraphenylporphyrin in dichloromethane according to the usual metallation procedure.[11]

Methods. ^{1}H and ^{13}C NMR spectra were recorded at 293 K, unless stated otherwise, in $CDCl_3$ with tetramethylsilane as internal standard using a Varian VXR-5000 400 MHz NMR spectrometer. Mass spectra of the porphyrins were recorded using a Finnigan Mat 1020B instrument [electron impact mass spectrometry (EI-MS)], a VG ZAB/HF analytical instrument [positive-ion fast atom bombardment (FAB) MS with 3-mercaptopropane-1,2-diol as matrix] or a VG AutoSpecQ instrument [positive field desorption (FD) MS]. Owing to decomposition of the compounds, no melting points could be obtained. Spectroscopic-grade dichloromethane was used for all photophysical measurements. Absorption and fluorescence spectra were recorded using a Varian Cary 210 spectrophotometer and a fully corrected Aminco spf 500 spectrofluorimeter. Fluorescence quantum yields are based on that of Rhodamine B in absolute ethanol ($\Phi_f = 0{\cdot}97$[18]). The solutions used for fluorescence measurements were deoxygenated by purging with

argon. Fluorescence lifetimes were determined with single-photon counting (SPC) equipment as described previously.[19] The data were deconvoluted in a global analysis with subsequent calculation of the species-associated spectra.[20] An excitation wavelength 420 nm was used in all the time-resolved fluorescence measurements and the fluorescence decays were measured at 587, 601, 632 and 656 nm. A liquid-nitrogen cryostat (Oxford Instruments DN 1704 with DTC2 temperature controller) was used for measurements at low temperatures.

Condensation of pyrrole with a 3:1 molar ratio of benzaldehyde and 4-bromobenzaldehyde. 4-Bromobenzaldehyde (15·46 g, 83 mmol) and freshly distilled benzaldehyde (25·5 ml, 0·25 mol) were added to boiling propionic acid (1·25 l, reagent grade). After 5 min, freshly distilled pyrrole (23 ml, 0·333 mol) was slowly added and the reaction mixture was refluxed for 30 min. Almost all the propionic acid was then removed through evaporation at reduced pressure and the black oily residue was dissolved in dichloromethane (250 ml). The resulting solution was washed with two portions of aqueous sodium hydroxide solution (2 × 100 ml, 0·1 M) and two portions of water (2 × 100 ml), dried over an hydrous magnesium sulphate and filtered through a short silica gel column to remove polymeric materials. The solution was concentrated to 150 ml and methanol (200 ml) was slowly added. The crystalline material obtained was filtered off and washed with methanol (200 ml). This gave 9·91 g (17%) of a nearly statistical mixture of six tetraphenylporphyrins, with about 40% contents of the desired 5-(4-bromophenyl)-10,15,20-triphenylporphyrin (**6**), and a small amount of the corresponding chlorins with zero to four bromo substituents: ^{1}H NMR (400 MHz, $CDCl_3$), δ 8·80–8·88 (8H, m, pyrrole-*H*), 8·18–8·24 (6H, m, Ar2-*H*), 8·05–8·10 [2H, m, (several overlapping doublets, $J \approx 8·7$ Hz), *p*-BrAr2-*H*], 7·86–7·91 [2H, m, (several overlapping doublets, $J \approx 8·7$ Hz), *p*-BrAr3-*H*], 7·71–7·81 (9H, m, Ar3-*H* and 4-*H*), −2·86 to −2·75 [2H, br m, (several overlapping broad singlets) pyrrole-N*H*]; ^{13}C NMR (100 MHz, $CDCl_3$), δ 142·37, 142·26, 141·36, 136·08, 134·77, 131 (vbr), 130·14, 130·10, 128·04, 127·99, 127·92, 126·93, 126·89, 122·5–123·0, 120–121.

5-(4-Formylphenyl)-10,15,20-triphenylporphyrin (**7**). The above mixture of bromo-substituted porphyrins (2·08 g, 3·0 mmol) was dissolved in dry diethyl ether (100 ml) and the solution was cooled to 0 °C. Butyllithium (1·6 M solution in hexane, 8·0 ml, 12 mmol) was added dropwise under argon and the reaction mixture was then stirred under argon at 0 °C for 2 h. Dry *N*,*N*-dimethylformamide (8·0 ml, 12 mmol) was added and after stirring for 30 min at 0 °C and an additional 30 min at ambient temperature, the reaction mixture was hydrolysed with 2 M hydrochloric acid. After neutralisation with sodium hydroxide the reaction mixture was extracted several times with dichloromethane and the combined organic extracts were washed with water and dried over anhydrous magnesium sulphate. After evaporation of the solvent the residue was purified by column chromatography on silica gel with dichloromethane as eluent to give 0·67 g (35%) of **7** contaminated with a few per cent of the corresponding chlorine. TLC (silica gel, CH_2Cl_2), $R_f = 0·46$; ^{1}H NMR (400 MHz, $CDCl_3$), δ 10·37 (1H, s, 5ArC*H*O), 8·88 (2H, d, $J = 4·8$ Hz, pyrrole-*H*), 8·86 (4H, s, pyrrole-*H*), 8·78 (2H, d, $J = 4·8$ Hz, pyrrole-*H*), 8·40 (2H, d, $J = 8·2$ Hz, 5Ar2-*H*), 8·26 (2H, d, $J = 8·2$ Hz 5Ar3-*H*), 8·18–8·24 (4H, m, 10,15,20Ar2-*H*), 7·70–7·81 (9H, m, 10,15,20Ar3-*H* and 4-*H*), −2·77 (2H, br s, pyrrole-N*H*); ^{13}C NMR (100 MHz, $CDCl_3$), δ 192·58, 148·91, 142·20, 142·18, 135·78, 135·40, 134·75, 131·5 (vbr), 128·23, 128·03, 127·00, 120·90, 120·70, 118·22; EI-MS, *m*/*z* (relative intensity, %) 642 (M^+, 71), 614 (19), 321 (M^{2+}, 48), 307 (100).

The formylated product (2·20 g, 3·4 mmol) prepared as described above was dissolved in toluene (1000 ml) and the mixture was heated to reflux. 2,3-Dichloro-5,6-dicyano-1,4-benzoquinone (0·5 g, 2·2 mmol) was added and the reaction mixture was refluxed for 30 min. The reaction mixture was cooled to room temperature and extracted with aqueous sodium hydroxide solution (1 l, 1%) containing sodium dithionite (1 g, 5·7 mmol). The organic layer was separated and washed with two portions of brine (2 × 300 ml) and three portions of water (3 × 300 ml) and dried over anhydrous sodium sulphate. Evaporation of the solvent gave 1·95 g (89%) of chlorin-free 5-(4-formylphenyl)-10,15,20-triphenylporphyrin: UV–visible absorption (CH_2Cl_2), λ_{max} (nm) 419, 515, 550, 590, 648.

5-(4-Hydroxymethylphenyl)-10,15,20-triphenylporphyrin (**8**). 5-(4-Formylphenyl)-10,15,20-triphenylporphyrin (1·93 g, 3·0 mmol) was dissolved in dry tetrahydrofuran (150 ml) and sodium borohydride (0·54 g, 12·0 mmol) was added. The reaction mixture was then refluxed for 1 h. After the reaction mixture had cooled to room temperature, water (75 ml) and aqueous sodium hydroxide solution (25 ml, 1 M) were added. The mixture was extracted with three portions of dichloromethane (3 × 75ml). The combined organic extracts were washed with two portions of brine (2 × 150 ml) and once with water (150 ml) and dried over anhydrous magnesium sulphate. Evaporation of the solvent gave 1·89 g (97%) of porphyrin **8**: ^{1}H NMR (400 MHz, $CDCl_3$), δ 8·85 (8H, br s, pyrrole-*H*), 8·18–8·26 (8H, m, 5,10,15,20Ar2-*H*), 7·69–7·81 (11H, m, 5,10,15,20Ar3-*H*, and 10,15,20Ar4-*H*), 5·04 (2H, br s, 5ArCH_2OH), −2·78 (2H, br s, pyrrole-N*H*); ^{13}C NMR (100 MHz, $CDCl_3$), δ 142·36, 141·75,

140·44, 134·95, 134·77, 131·5 (vbr), 127·93, 126·90, 125·52, 120·37, 119·96, 65·61; EI-MS, *m/z* (relative intensity, %) 644 (M^+, 78), 628 (22), 614 (18), 322 (M^{2+}, 52), 314 (40), 307 (100).

5-(4-Bromomethylphenyl)-10,15,20-triphenylporphyrin (**9**). 5-(4-Hydroxymethylphenyl)-10,15,20-triphenylporphyrin (1·87 g, 2·9 mmol) was suspended in hydrobromic acid (150 ml, 30% in glacial acetic acid) and refluxed for 2 h. After the reaction mixture had cooled to room temperature it was poured into ice–water (150 g). The mixture was neutralized with sodium hydroxide solution (450 ml, 5 M) and extracted with three portions of dichloromethane (3 × 150 ml). The combined organic layers was washed with water (200 ml) and dried over magnesium sulphate. Evaporation of the solvent gave 2·0 g (99%) of porphyrin **9**: ^{1}H NMR (400 MHz, $CDCl_3$), δ 8·81–8·87 (8H, m, pyrrole-*H*), 8·19–8·25 (6H, m, 10,15,20Ar2-*H*), 8·18 (2H, d, *J* = 8·0 Hz, 5Ar2-*H*) 7·70–7·79 (11H, m, 5,10,15,20Ar3-*H* and 10,15,20Ar4-*H*), 4·82 (2H, s, 5ArCH_2Br) −2·78 (2H, br s, pyrrole-N*H*); ^{13}C NMR (100 MHz, $CDCl_3$), δ 142·58, 142·31, 137·45, 135·12, 134·77, 131·2 (vbr), 127·95, 127·63, 126·91, 120·54, 120·45, 119·37, 33·76; EI-MS, *m/z* (relative intensity, %) 706 (M^+, 1), 628 (9), 614 (4), 314 (15), 307 (8), 82 (88), 81 (50), 80 (100), 79 (85).

Zinc 5-(4-bromomethylphenyl)-10,15,20-triphenylporphyrin (**10**). 5-(4-Bromomethylphenyl)-10,15,20-triphenylporphyrin (0·78 g, 1·1 mmol) was dissolved in dichloromethane (150 ml). Zinc acetate dihydrate (0·37 g, 1·68 mmol) dissolved in methanol (20 ml) was added and the mixture was refluxed under argon for 30 min. The reaction mixture was cooled to room temperature and washed with three portions of water (3 × 200 ml) and the organic layer was dried over sodium sulphate. Evaporation of the solvent gave 0·84 g (99%) of zinc porphyrin **10**: ^{1}H NMR (400 MHz, $CDCl_3$), δ 8·92–8·97 (8H, m, pyrrole-*H*), 8·18–8·24 (8H, m, 5,10,15,20Ar2-*H*), 7·71–7·80 (11H, m, 5,10,15,20Ar3-*H* and 10,15,20Ar4-*H*), 4·85 (2H, s, 5ArCH_2Br); ^{13}C NMR (100 MHz, $CDCl_3$), δ 150·49, 150·46, 150·43, 150·20, 143·24, 142·94, 137·23, 134·98, 134·63, 132·35, 132·30, 132·04, 127·75, 127·52, 126·79, 121·54, 121·46, 110·41, 33·89.

Compound **1**. 4,13-Diaza-18-crown-6 (**4**) (0·052 g, 0·2 mmol) and finely powdered sodium hydroxide (0·090 g, 2·25 mmol) were dissolved in water (1 ml). 5-(4-Bromomethylphenyl)-10,15,20-triphenylporhyrin (0·290 g, 0·41 mmol) was dissolved in chloroform (2 ml) and added dropwise with vigorous stirring. The reaction mixture was kept in the dark with vigorous stirring for 16 h. The organic layer was separated, diluted with chloroform (25 ml) and washed with three portions of water (3 × 15 ml). The organic layer was dried over sodium sulphate and evaporated on a rotary evaporator. The crude product was dissolved in a small amount of chloroform and loaded on to an aluminium oxide column. The product was eluted with chloroform (stabilized with 0·6% w/w ethanol) to give 0·199 g (66%) of compound **1**. TLC [aluminium oxide, $CHCl_3$ (stabilized with 0·6% w/w ethanol)], R_f = 0·30; ^{1}H NMR (400 MHz, $CDCl_3$), δ 8·79–8·89 (16H, m, pyrrole-*H*), 8·17–8·24 (12H, m, 10,15,20Ar2-*H*), 8·14 (4H, d, *J* = 8·0 Hz, 5Ar2-*H*), 7·65–7·78 (22H, m, 5,10,15,20Ar3-*H* and 10,15,20Ar4-*H*), 4·05 (4H, s, 5ArCH_2N), 3·86 (8H, t, *J* = 11·2 Hz, NCH_2CH_2O), 3·78 (8H, s, OCH_2CH_2O), 3·12 (8H, br t, *J* = 11·2 Hz, NCH_2CH_2O), −2·77 (4H, s, pyrrole-N*H*); ^{13}C NMR (100 MHz, $CDCl_3$), δ 142·83, 141·33, 139·91, 135·22, 131·5 (vbr), 128·34, 127·85, 127·35, 127·33, 120·88, 120·77, 120·72, 71·59, 70·94, 60·70, 54·82; FAB-MS, *m/z* (relative intensity, %) 1520 ($[M+5]^+$, 8), 1519 ($[M+4]^+$, 17), 1518 ($[M+3]^+$, 31), 1517 ($[M+2]^+$, 43), 1516 ($[M+1]^+$, 46), 1515 (M^+, 11), 1514 (9), group of peaks with the most intense peak at 889 (16), group of peaks with the most intense peak at 627 (100); UV–visible absorption (CH_2Cl_2), λ_{max} (nm) 417, 514, 549, 590, 647; fluorescence emission (λ_{ex} = 548 nm, CH_2Cl_2), λ_{max} (nm) 654, 720.

Compound **2**. 4,13-Diaza-18-crown-6 (**4**) (0·052 g, 0·2 mmol) and finely powdered sodium hydroxide (0·090 g, 2·25 mmol) were dissolved in water (1 ml). Zinc porphyrin **10** (0·339 g, 0·44 mmol) dissolved in chloroform (3·5 ml) was added dropwise with vigorous stirring. The reaction mixture was kept in the dark at ambient temperature with vigorous stirring for 40 h. Chloroform (10 ml) and water (10 ml) were added to the reaction mixture. The organic layer was separated and washed with five portions of water (5 × 10 ml) and dried over sodium sulphate. The solvent was evaporated on a rotary evaporator and the crude product was dissolved in a small amount of dichloromethane and loaded on to an aluminium oxide column prepared in dichloromethane. Two bands were eluted with 0·5% CH_3OH, 1% pyridine–CH_2Cl_2. The substance from the second band was further purified by column chromatography on an aluminium oxide column. The product was eluted as the first band with chloroform (stabilized with 0·6% w/w ethanol). In this way 0·175 g (53%) of **2** was obtained: ^{1}H NMR (400 MHz, $CDCl_3$, *ca* 1×10^{-2} M, 328 K), δ 8·87–8·93 (16H, m, pyrrole-*H*), 8·16–8·22 (12H, m, 10,15,20Ar2-*H*), 8·09 (4H, d, *J* = 8 Hz, 5Ar2-*H*), 7·65–7·76 (18H, m, 10,15,20Ar3-*H* and 4-*H*), 7·61 (4H, d, *J* = 8 Hz, 5Ar3-*H*), 3·89 (4H, br s, 5ArCH_2N), 3·56 (8H, br t, *J* = 6 Hz, NCH_2CH_2O), 3·44 (8H, br s, OCH_2CH_2O), 2·86 (8H, br t, *J* = 6 Hz, NCH_2CH_2O); ^{13}C NMR (100 MHz, $CDCl_3$, *ca* 1×10^{-2} M), δ 150·36, 150·28, 143·37, 141·66, 138·5 (br), 134·76, 134·59, 132·13, 132·01,

127·49, 126·92, 126·66, 122·31, 121·16, 121·00, 120·93, 69·5 (br), 69·0 (br), 59·0 (br), 53·33, 29·93; FD-MS, *m/z* (relative intensity, %) 1649 ($[M+10]^+$, 9), 1648 ($[M+9]^+$, 18), 1647 ($[M+8]^+$, 32), 1646 ($[M+7]^+$, 49), 1645 ($[M+6]^+$, 72), 1644 ($[M+5]^+$, 92), 1643 ($[M+4]^+$, 100), 1642 ($[M+3]^+$, 89), 1641 ($[M+2]^+$, 90), 1640 ($[M+1]^+$, 59), 1639 (M^+, 50), group of peaks with the most intense peak at 951 (18), 824 ($[M+10]^{2+}$, 3), 824 ($[M+9]^{2+}$, 7), 823 ($[M+8]^{2+}$, 13), 823 ($[M+7]^{2+}$, 17), 822 ($[M+6]^{2+}$, 22), 822 ($[M+5]^{2+}$, 28), 821 ($[M+4]^{2+}$, 35), 821 ($[M+3]^{2+}$, 31), 820 ($[M+2]^{2+}$, 29), 820 ($[M+1]^{2+}$, 20), 819 (M^{2+}, 18), group of peaks with the most intense peak at 690 (10); UV–visible absorption (CH_2Cl_2), λ_{max} (nm) 419, 547, 584; fluorescence emission (λ_{ex} = 548 nm, CH_2Cl_2), λ_{max} (nm) 598, 646

Compound **5**. 4,13-Diaza-18-crown-6 (**4**) (0·708 g, 2·7 mmol) and finely powdered sodium hydroxide (0·486 g, 12·1 mmol) were dissolved in water (13·5 ml). Porphyrin **9** (0·405 g, 0·57 mmol) dissolved in chloroform (45 ml) was added with vigorous stirring and the reaction mixture was kept in the dark with vigorous stirring for 40 h. The organic layer was separated and washed with three portions of dilute hydrochloric acid (3 × 15 ml, 0·1 M) and four portions of water (4 × 25 ml) and dried over sodium sulphate. The solvent was removed under reduced pressure and the crude product was dissolved in a small amount of dichloromethane and loaded on to an aluminium oxide column prepared in dichloromethane. Three bands were eluted with 0·5% CH_3OH, 1% pyridine–CH_2Cl_2 and a fourth band, the product, was eluted with 5% CH_3OH–CH_2Cl_2. The product was further purified by column chromatography on a freshly prepared Sephadex LH-20 column using pyridine as eluent. The main body of the first band was collected. In this way 0·310 g (65%) of **5** was obtained: ^{1}H NMR (400 MHz, $CDCl_3$), δ 8·82–8·88 (8H, m, pyrrole-*H*), 8·18–8·24 (6H, m, 10,15,20Ar2-*H*), 8·15 (2H, d, *J* = 7·6 Hz, 5Ar2-*H*), 7·66–7·80 (11H, m, 5,10,15,20Ar3-*H* and 10,15,20Ar4-*H*), 4·05 (2H, br s, 5ArCH_2N), 3,82 (4H, br t, *J* = 5·6 Hz, NCH_2CH_2O), 3·62–3·73 (12H, m, $OCH_2CH_2OCH_2CH_2NH$), 3·07 (4H, br t, *J* = 5·6 Hz, NCH_2CH_2O), 2·83 (4H, br t, *J* = 4·6 Hz, OCH_2CH_2NH), 2·10 (1H, vbr s, N*H*), −2·78 (4H, br s, pyrrole-N*H*); ^{13}C NMR (100 MHz, $CDCl_3$), δ 142·39, 142·37, 140·78, 139·56, 134·77, 134·73, 131 (vbr), 127·90, 127·37, 126·88, 120·49, 120·30, 120·25, 71·19, 70·59, 70·53, 70·40, 59·93, 54·16, 49·60.

Compound **3**. A solution of compounds **5** (0·310 g, 0·35 mmol) and **10** (0·296 g, 0·38 mmol) dissolved in chloroform (7·0 ml) was added to a vigorously stirred solution of sodium hydroxide (0·088 g, 2·20 mmol) in water (1·5 ml). The reaction mixture was kept in dark with vigorous stirring for 40 h. Chloroform (15 ml) and water (15 ml) were added to the reaction mixture. The organic layer was separated, washed with five portions of water (5 × 15 ml) and dried over sodium sulphate. The solvent was removed on a rotary evaporator and the crude product was dissolved in a small amount of dichloromethane and loaded on to an aluminium oxide column. One small band was first eluted with dichloromethane and then a second strong band was eluted with 0·5% CH_3OH, 1% pyridine–CH_2Cl_2. The substance from the second band was then further purified on a freshly prepared Sephadex LH-20 column using pyridine as eluent. Three bands were obtained, one very strong, thick, purple band followed by two pale, thin bands. The substance from the first band was again purified by column chromatography on an aluminium oxide column. Two pale, thin bands were eluted with chloroform (stabilized with 0·6% w/w ethanol) and a third strong band was eluted with 0·25% C_2H_5OH–$CHCl_3$ (stabilized with 0·6% w/w ethanol) to give 0·254 g (46%) of **3**: ^{1}H NMR (400 MHz, $CDCl_3$, *ca* 1 × 10^{-2} M, 323 K), δ 8·87–8·92 (8H, m, pyrrole-*H*[Zn]), 8·78–8·83 (8H, m, pyrrole-*H*), 8·15–8·22 (12H, m, 10,15,20Ar2-*H* and 10,15,20Ar[Zn]2-*H*), 8·12 (2H, d, *J* = 8 Hz, 5Ar[Zn]2-*H*), 8·11 (2H, d, *J* = 8 Hz, 5Ar2-*H*), 7·63–7·77 (22H, m, 5,10,15,20Ar3-*H*, 5,10,15,20Ar[Zn]3-*H*, 10,15,20Ar4-*H* and 10,15,20Ar[Zn]4-*H*), 3·98 (4H, br s, 5ArCH_2N and 5Ar[Zn]CH_2N), 3·73 (8H, br t, *J* = 5 Hz, NCH_2CH_2O), 3·64 (8H, s, OCH_2CH_2O), 2·96–3·04 (8H, br m, NCH_2CH_2O), −2·72 (2H, br s, pyrrole-N*H*), ^{13}C NMR (100 MHz, $CDCl_3$, *ca* 1 × 10^{-2} M 323 K), δ 150·58, 150·49, 143·42, 142·56, 141·00, 134·80, 134·75, 132·07 (br), 131·3 (vbr), 127·91, 127·60, 127·37, 127·20, 126·88, 126·67, 121·30, 121·19, 121·15, 120·50, 120·35, 120·31, 71·18, 70·60, 60·44, 60·39, 54·63; FAB-MS, *m/z* (relative intensity, %) 1585 ($[M+8]^+$, 8), 1584 ($[M+7]^+$, 18), 1583 ($[M+6]^+$, 30), 1582 ($[M+5]^+$, 43), 1581 ($[M+4]^+$, 48), 1580 ($[M+3]^+$, 57), 1579 ($[M+2]^+$, 56), 1578 ($[M+1]^+$, 65), group of peaks with the most intense peak at 889 (18), group of peaks with the most intense peak at 689 (86), group of peaks with the most intense peak at 628 (100); UV–visible absorption (CH_2Cl_2), λ_{max} (nm) 419, 515, 549, 589, 647; fluorescence emission (λ_{ex} = 548 nm, CH_2Cl_2), λ_{max} (nm) 598, 652, 720.

ACKNOWLEDGEMENTS

We thank Dr B. Albinsson and Mr A. Holmén, Department of Physical Chemistry, Chalmers University of Technology, for helpful discussions. Financial support from the Swedish Natural Science Research Council and the Swedish Research Council for Engineering Sciences is gratefully acknowledged.

REFERENCES

1. (a) T. Förster, *Ann. Phys. (Leipzig)*, **2**, 55–75 (1948); (b) T. Förster, *Z. Naturforsch., Teil A* **4**, 321–327 (1949); (c) T. Förster, *Discuss. Faraday Soc.* **27**, 7–17 (1959).
2. (a) D. L. Dexter, *J. Chem. Phys.* **21**, 836–850 (1953); (b) M. Inokuti and F. Hirayama, *J. Chem. Phys.* **43**, 1978–1989 (1965).
3. L. Stryer and R. P. Haugland, *Proc. Natl Acad. Sci. USA*, **58**, 719–726 (1967).
4. A. Osuka, K. Maruyama, I. Yamazaki and N. Tamai, *Chem. Phys. Lett.* **165**, 392–396 (1990).
5. R. P. Haugland, J. Yguerabide and L. Stryer, *Proc. Natl Acad. Sci. USA*, **63**, 23–30 (1969).
6. (a) H. Oevering, J. W. Verhoeven, M. N. Paddon-Row, E. Cotsaris and N. S. Hush, *Chem. Phys. Lett.* **143**, 488–495 (1988); (b) J. Kroon, A. M. Oliver, M. N. Paddon-Row and J.W. Verhoever, *J. Am. Chem. Soc.* **112**, 4868–4873 (1990).
7. T. Lyoda, M. Morimoto, N. Kawasaki and T. Shimidzu, *J. Chem. Soc., Chem. Commun.* 1480–1481 (1991).
8. J. Mårtensson, K. Sandros and O. Wennerström, *Tetrahedron Lett.* **34**, 541–544 (1993).
9. A. D. Adler, F. R. Longo, J. D. Finarelli, J. Goldmacher, J. Assour and L. Korsakoff, *J. Org. Chem.* **32**, 476 (1967).
10. (a) G. H. Barnett, M. F. Hudson and K. M. Smith, *Tetrahedron Lett.* 2887–2888 (1973); (b) K. Rousseau and D. Dolphin, *Tetrahedron Lett.* 4251–4254 (1974).
11. J.-H. Fuhrhop and K. M. Smith, *Porphyrins and Metalloporphyrins*, Chapt. 19. Elsevier, New York (1975).
12. (a) M. Kasha, H. R. Rawls and M. A. El. Bayoumi, *Pure Appl. Chem.* **11**, 371–392 (1965); (b) J. H. Sharp and M. Lardon, *J. Phys. Chem.* **72**, 3230–3235 (1968); (c) M. Gouterman, D. Holten and E. Lieberman, *Chem. Phys.* **25**, 139–153 (1977); (d) R. Selensky, D. Holten, M. W. Windsor, J. B. Paine, III, D. Dolphin, M. Gouterman and J. C. Thomas, *Chem. Phys.* **60**, 33–46 (1981); (e) A. Osuka and K. Maruyama, *J. Am. Chem. Soc.* **110**, 4454–4456 (1988); (f) C. A. Hunter, J. K. M. Sanders and A. J. Stone, *Chem. Phys.* **133**, 395–404 (1989); (g) G. A. Schick, I. C. Schreiman, R. W. Wagner, J. S. Lindsey and D. F. Bocian, *J. Am. Chem. Soc.* **111**, 1344–1350 (1989); (h) D. E. LaLonde, J. D. Petke and G. M. Maggiora, *J. Phys. Chem.* **93**, 608–614 (1989); (i) S. Eriksson, B. Källebring, S. Larsson, J. Mårtensson and O. Wennerström, *Chem. Phys.* **146**, 165–177 (1990).
13. R. L. Brookfield, H. Ellul, A. Harriman and G. Porter, *J. Chem. Soc., Faraday Trans. 2* **82**, 219–223 (1986).
14. K. A. Arnold, A. M. Viscariello, M. Kim, R. D. Gandour, F. R. Fronczek and G. W. Gokel, *Tetrahedron Lett.* **29**, 3025–3028 (1988).
15. J. A. Anton, P. A. Loach and Govindjee, *Photochem. Photobiol.* **28**, 235–242 (1978).
16. (a) K. N. Solov'ev, *Opt. Spectrosc.* **10**, 389–393 (1961); (b) G. P. Gurinovich, A. N. Sevchenko and K. N. Solov'ev, *Opt. Spectrosc.* **10**, 396–401 (1961); (c) M. Gouterman and L. Stryer, *J. Chem. Phys.* **37**, 2260–2266 (1962).
17. A. D. Adler, F. R. Longo and V. Varadi, *Inorg. Synth.* **15**, 213–220 (1975).
18. G. Weber and F. W. J. Teale, *Trans. Faraday Soc.* **53**, 646–655 (1957).
19. J.-E. Löfroth, PhD Thesis, University of Göteborg (1982).
20. J.-E. Löfroth, *Anal. Instrum.* **14**, 403–431 (1985); *J. Phys. Chem.* **90**, 1160–1168 (1986).